

In this document, the reviewer comments are in black, the authors responses are in red.

The authors thank the reviewer for their detailed review and useful suggestions to improve the quality of our work.

In this manuscript, a technique to measure turbulence dissipation rate from Doppler lidar observations is presented using data collected from several Doppler lidars during XPIA. The dissipation rates are compared with those from sonic anemometers for verification (and to determine the sample length for the best agreement). Statistics of dissipation are presented for the experiment, which serve as a brief climatology of dissipation at the site.

The manuscript is generally written and organized well, and results in this manuscript are of significant interest to a wide audience in the Doppler lidar and boundary-layer fields. Still, there are some significant omissions in the description of the technique and how the presented results are interpreted. As such, I recommend that this manuscript be reconsidered for publication after major revisions, after the following concerns have been addressed.

Thank you for finding our results interesting!

General/major comments:

- a) How exactly is the turbulence dissipation calculated using the Doppler lidar data? More details need to be added to Sect. 3.2 so that this technique could be applied by a reader. From the Halo data, it must be the vertical staring observations. From the V1/V2 profiler data, which beam position is used (and why)? Was dissipation calculated from each beam separately, and the mean of those used?

While isotropy is assumed, turbulence is rarely isotropic in the boundary-layer, especially under stable conditions when turbulent eddies are more horizontally oriented. As such, there could be differences (particularly with the Halo which just uses vertical beam) between the lidar estimates and sonic anemometer estimates (which use the horizontal variance alone) from anisotropy. This should be briefly discussed.

The description of the method in Section 3.2 now includes the following sentences, which also briefly comment the assumption of isotropic turbulence:

“For the WINDCUBE lidars, the variance of the observed line-of-sight velocity σ_v^2 can be calculated as average from all the beams. In doing so, we include turbulence contributions from both the horizontal and vertical dimensions, and we make the limiting (Kaimal et al. 1972, Mann 1994) assumption of isotropic turbulence. For the Halo Streamline lidar, which operated in a vertical stare mode, σ_v^2 is calculated from the vertically pointing beam, and therefore ϵ will strictly include turbulence contributions only in the vertical dimension, thus possibly determining different values compared to what is retrieved from the WINDCUBE lidars. Another difference due to the different scan patterns used by the

considered lidars is related to the determination of the horizontal wind speed U . For the WINDCUBE lidars, U can be derived from the line-of-sight velocity measurements from the different beams, with the assumption of horizontal homogeneity of the flow over the probed volume. In the case of the Halo Streamline, no information about the horizontal wind can be derived from the measurements in the vertical staring mode, which only measures the vertical component of the wind speed. U is then retrieved from a sine-wave fitting from the VAD scans that are performed every 12 min”.

Moreover, we have added and modified the following sentences in Section 4, to emphasize again the differences between the results from the different instruments:

“It is reasonable to explain the higher error ($\sim +10\%$) of the Halo Streamline compared to the WINDCUBE lidars at 100m AGL as a consequence of the differences in the spatial dimensions that are samples by the two lidars. While the lidar beams of the WINDCUBE are tilted, and they therefore include turbulence contributions in the horizontal dimension (which is the only contribution considered in the determination of ϵ from the sonic anemometers), ϵ from the Halo Streamline is only retrieved using information from the vertically pointing beams. Moreover, the necessary approximations adopted in the determination of the horizontal velocity U for the Halo Streamline lidar, as explained in Section 3.2, likely determine an additional error increase for this lidar.”

References:

- Mann, J., 1994. *The spatial structure of neutral atmospheric surface-layer turbulence. Journal of fluid mechanics*, 273, pp.141-168.
- Kaimal, J.C., Wyngaard, J.C.J., Izumi, Y. and Coté, O.R., 1972. *Spectral characteristics of surface-layer turbulence. Quarterly Journal of the Royal Meteorological Society*, 98(417), pp.563-589.

- b) In Sect. 4, the sampling length for calculation of dissipation during stable, neutral, and unstable conditions is chosen as the minimum of the MAE between the sonic and lidar estimate. This is fine when there is sonic anemometer data for both verification and classifying stability, but most sites that this technique could be applied to will not have coincident sonic measurements. How could this technique be applied to other sites, where the turbulence characteristics/stability might be quite different? This is a major limiting factor in the applicability of this technique, and currently there is no discussion of how this could be applied to other sites given this limitation. Also, does the minimum in the MAE vary between slightly stable and strongly stable conditions, when the inertial subrange may be much smaller? Should the analysis in Fig. 5 be done with more stability classifications (strongly stable/unstable, weakly stable/unstable, neutral)? Perhaps this technique could be refined so that the sample length varies with the outer scale of the inertial subrange, as determined from the Doppler lidar data alone. Then, the technique could be easily applied to other lidar data. Alternatively, the authors could add a short section (a few paragraphs)

on how this technique could be applied at locations without sonic anemometer data for stability and determination of the sample length to use.

We have refined our approach to propose an alternative to use when measurements from co-located sonic anemometers are not available. We have included in the manuscript the following additional subsection:

4.1 Determination of the optimal time scales to retrieve ϵ from lidars in absence of co-located sonic anemometers

The availability of multiple sonic anemometers co-located with the lidars at XPIA has allowed for a direct comparison between ϵ estimates from different instruments to determine the optimal length scales, in different stability conditions, to use when retrieving ϵ from Doppler lidar measurements. This approach does not require the direct calculation of spectra from the line-of-sight velocity measured by the lidars, and therefore it represents a time-efficient technique. However, the proposed method is only viable when sonic anemometers are deployed in the near vicinity of a lidar, and when measures of atmospheric stability are available.

When a comparison with sonic anemometer data is not possible, the appropriate time scale to use in the lidar retrieval of ϵ can be determined by finding the maximum wavelength within the inertial sub-range in the velocity spectra from the lidar measurements. To do so, spectral models can be fitted to the observed spectra. Several models have been proposed for turbulence spectra in different stability conditions (Kaimal et al., 1972; Panofsky, 1978; Olesen et al., 1984). We test the spectral model proposed by Kristensen et al. (1989), which proposes expressions for both the cases of an isotropic and an anisotropic horizontally homogeneous flow. To validate our results and test this alternative approach to derive ϵ from lidar measurements, we use data from the Halo Streamline lidar to estimate the maximum wavelength λ_z within the inertial subrange. Since the Halo mainly operated in a vertical stare mode during XPIA, we consider the following expression for the turbulence spectrum of the vertical component of the wind speed:

$$S(k) = \frac{\sigma_z^2 l_z}{2\pi} \frac{1 + \frac{8}{3} \left(\frac{l_z k}{a(\mu)} \right)^{2\mu}}{\left[1 + \left(\frac{l_z k}{a(\mu)} \right)^{2\mu} \right]^{5/(6\mu)+1}} \quad (16)$$

where k is the wavenumber, σ_z is the standard deviation of the vertical component of the wind speed used to compute the spectrum, l_z is the integral scale of the vertical velocity along the horizontal flow trajectory, and the parameter μ controls the curvature of the spectrum. We use $\mu = 1.5$, which provides a good match with our experimental spectra, as also found in previous studies (Lothon et al., 2009; Tonttila et al., 2015). The parameter a can be expressed as a function of μ as:

$$a(\mu) = \pi \frac{\mu \Gamma\left(\frac{5}{6\mu}\right)}{\Gamma\left(\frac{1}{2\mu}\right) \Gamma\left(\frac{1}{3\mu}\right)} \quad (17)$$

We calculate spectra using 10-min consecutive data, and we fit the spectral model to the experimental data, leaving out frequencies greater than 0.2Hz, which are affected by instrumental noise (Frehlich, 2001), not modeled here. An example of a measured spectrum and the fit resulting from the model are shown in Figure 9. The transition wavelength λ_z between the

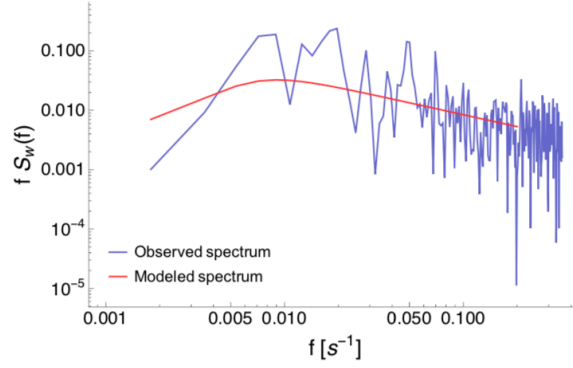


Figure 9. Example of power spectral density of the vertical component of the wind speed as measured by the Halo Streamline lidar on 11 March 2015 18:05 UTC. The red line represents the fit according to the spectral model from Eq. (16).

inertial sub-range and the outer scales can be expressed as a function of the integral scale l_z and the parameter μ :

$$\lambda_z = \left[\frac{5}{3} \sqrt{\mu^2 + \frac{6}{5}\mu + 1} - \left(\frac{5}{3}\mu + 1 \right) \right]^{1/(2\mu)} \frac{2\pi}{a(\mu)} l_z \quad (18)$$

Following the approach in Tonttila et al. (2015), we estimate the timescale corresponding to this transition wavelength by dividing λ_z by the collocated wind speed derived from the closest PPI scan performed by the Halo Streamline lidar.

To compare the results from this approach with what we obtain from the comparison with dissipation rates from the sonic anemometer data, we apply this technique to the data from the Halo Streamline for the whole period of XPIA, and calculate the average timescales for different stability conditions at 100m AGL. We obtain an average time scale of 32s in stable conditions, and 73s in unstable conditions. Both these values compare well with what is found with the more time-efficient comparison with the sonic anemometer retrievals (values in Table 2), thus confirming that the use of spectral models can be considered a valid alternative for the determination of the optimal sample lengths to retrieve ϵ from lidar data.

The use of spectral models to determine the appropriate sample size to use when retrieving ϵ from lidars can also be applied when information about atmospheric stability are not available or accurate. In these cases, instead of calculating an average optimal sample size for each stability condition, an appropriate time scale can be determined at each time ϵ is retrieved from lidar measurements, from a single spectrum. We compare ϵ values from the sonic anemometers and from the Halo Streamline lidar, with the optimal time scales obtained from both the proposed approaches (comparison with the sonic anemometer data and analysis of instantaneous spectra) in Figure 10, for the same time period shown in Figure 7. The use of spectral models to determine the extension of the inertial sub-range in the lidar spectra produces valid estimates of ϵ : for this case we obtain a MAE= 0.40, and a correlation coefficient $R^2 = 0.78$.

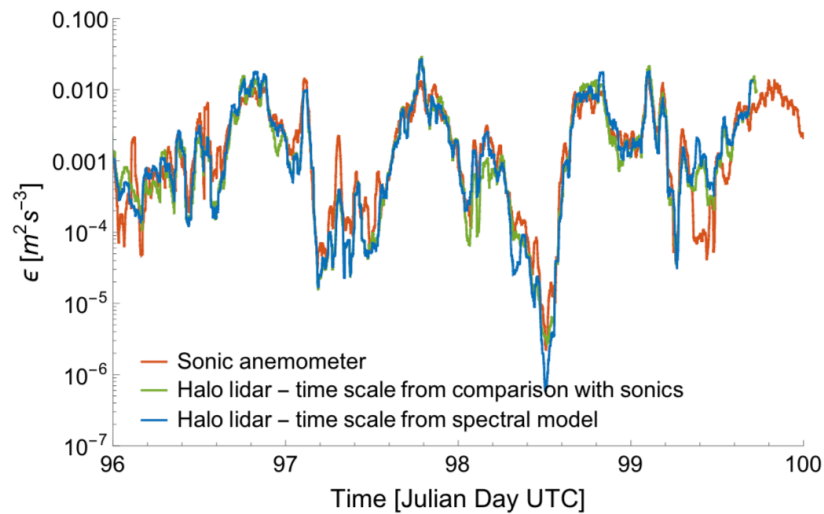


Figure 10. Time series from 6 April 2015 00 UTC to 10 April 2015 00 UTC comparing ϵ from sonic anemometers and the Halo Streamline lidars at 100m AGL, where the time scales for the lidars have been determined with both the proposed approaches (comparison with ϵ from sonic anemometers and fit with spectral models). Data have been smoothed with a 30-min running mean.

References:

- Caughey, S.J. and Palmer, S.G., 1979. Some aspects of turbulence structure through the depth of the convective boundary layer. *Quarterly Journal of the Royal Meteorological Society*, 105(446), pp.811-827.
- Kaimal, J.C., Wyngaard, J.C.J., Izumi, Y. and Coté, O.R., 1972. Spectral characteristics of surface-layer turbulence. *Quarterly Journal of the Royal Meteorological Society*, 98(417), pp.563-589.
- Kristensen, L., Lenschow, D.H., Kirkegaard, P. and Courtney, M., 1989. The spectral velocity tensor for homogeneous boundary-layer turbulence. In *Boundary Layer Studies and Applications* (pp. 149-193). Springer, Dordrecht.
- Lothon, M., Lenschow, D.H. and Mayor, S.D., 2009. Doppler lidar measurements of vertical velocity spectra in the convective planetary boundary layer. *Boundary-layer meteorology*, 132(2), pp.205-226.
- Olesen, H.R., Larsen, S.E. and Højstrup, J., 1984. Modelling velocity spectra in the lower part of the planetary boundary layer. *Boundary-Layer Meteorology*, 29(3), pp.285-312.
- Panofsky, H.A., 1978. Matching in the convective planetary boundary layer. *Journal of the Atmospheric Sciences*, 35(2), pp.272-276.
- Tonttila, J., O'Connor, E.J., Hellsten, A., Hirsikko, A., O'Dowd, C., Järvinen, H. and Räisänen, P., 2015. Turbulent structure and scaling of the inertial subrange in a stratocumulus-topped boundary layer observed by a Doppler lidar. *Atmospheric chemistry and physics*, 15(10), pp.5873-5885.

Specific comments:

- a) p. 2 line 5; p. 21 line 27: Here, the authors make the case that both production and dissipation of TKE need to be known for turbulence closure. The authors state that by measuring dissipation, the scales at which the assumption of local equilibrium are broken will be assessed. However, in order to do this, production must also be measured. The authors should add a few statements on how production of TKE can be measured for the full closure.

We agree that TKE production needs to be calculated in order to have a full closure of the TKE budget. Since the focus of this work is on determining the variability of turbulence dissipation, which itself has an extreme importance as shown in Yang et al. 2017, we have decided to leave out from this manuscript the reference to the determination of the scales at which the assumption of local equilibrium breaks. As a consequence, we have deleted from the introduction the sentence “in order to understand at what spatio-temporal scale local imbalance becomes important.” We have also deleted from the conclusions the sentence “the scales at which the assumption of local equilibrium is broken will be assessed”.

- b) Figure 1 caption: Would be good to clarify that contours in the right panel are in m.

The caption of the figure now includes: “Contours in the right panel show elevation in m ASL.”

- c) p 3 line 1: Spell out XPIA in full here, for those unfamiliar with the project.

We have included “eXperimental Planetary boundary layer Instrumentation Assessment” in the revised version.

- d) p. 4, line 2: Was this sonic also a CSAT3 or was it different? If it was a different type of sonic, are there differences in the design that may cause the observed dissipation to be much higher than for CSAT 3 (possibly more obstructions, if it’s an RM Young anemometer) as later discussed in Sect. 5? Given its importance to the results, more details should be provided about this sonic, its siting, and any QC applied to it (was any data thrown out when it was waked by what it was mounted on)?

The sonic at 5m AGL was a CSAT3 as well. The description of this instrument in Section 2.1 is now as follows: “An additional sonic anemometer was mounted on a 5-m AGL surface flux station located 200 m south-west of the BAO tower over natural arid grassland. The sonic anemometer (Campbell CSAT3A) at this location operated with a frequency of 10 Hz.” The location of this 5m sonic anemometer is now included in the map in Figure 1.

- e) Table 1: Can the pulse width (FWHM) be added as a row to this table, as well? This will be useful in understanding the smallest eddies that can be resolved by a given lidar.

The Table now includes the pulse width for the instruments: 200ns for the WINDCUBE v1s, 175ns for the WINDCUBE v2, 150ns for the Halo Streamline.

- f) p. 5 line 19: How did the measured dissipation rates between the two sonic anemometers compare to each other when both were unwaked? Were they often similar, or were there often substantial differences? This might be useful to form a ‘baseline’ estimate of how much uncertainty is in any dissipation measurement from the sonic anemometers themselves.

We have compared dissipation rates from the two sonics (at each of the 6 heights of the BAO tower), and added the following sentences at the end of Section 3.1:

“As already mentioned, data were excluded for wind directions waked by the tower. When neither of the two anemometers is affected by tower wakes, ϵ is defined as the average between the two independent values obtained from the two sonics at each height. To quantify the uncertainty in turbulence dissipation rate measurements from the sonic anemometers, we have compared ϵ from the two sonics at each level when neither one was influenced by the tower wake. For each tower boom direction (northwest and southeast), we calculate the median absolute error (MAE) between ϵ from the sonic anemometers mounted on the considered boom direction and the correspondent average value from the two sonics:

$$MAE = median\left(\frac{|\epsilon_{single} - \epsilon_{average}|}{\epsilon_{average}}\right)$$

In calculating the error, we consider data from all heights, as no significant difference was noticed at different levels. For both the boom directions, we find very similar results, with $MAE = 0.19$, which is reduced to 0.14 when a 30-min running mean is applied to the ϵ time series. The distributions of the errors are included in the Supplementary Material. No bias was detected between the retrievals from the sonic anemometers on the two boom directions.”

We have also included the following plots in the Supplementary Material:

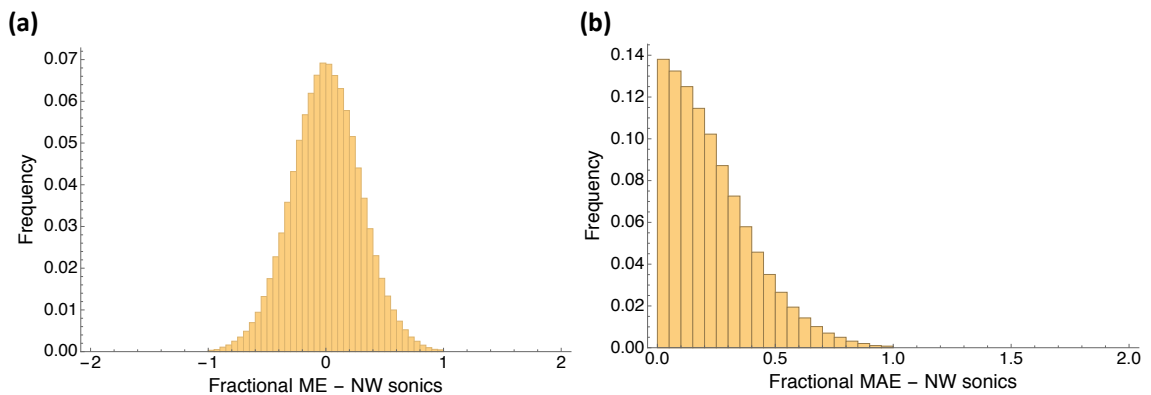


Figure S2: (a) histogram of the fractional median error between turbulence dissipation rate calculated from the sonic anemometers on the northwest booms and the average

dissipation from both the boom directions. Results for the sonic anemometers on the southeast booms are similar. (b) as in (a), but median absolute error. Raw values of ϵ are used.

- g) Eq. 5: By using this equation to estimate dissipation, it is implicitly assumed that the line-of-sight atmospheric variance (σ_w^2 in Eq. 8) is strictly the result of turbulent motion. However, non-turbulent motions such as gravity waves in a stable layer may increase the line-of-sight variance but are not turbulent, thus there is little dissipation with them. Under these conditions, turbulence dissipation would be overstated. This may be especially important at the BAO for westerly winds, due to the close presence of mountains to the west that may induce mountain waves when the atmospheric conditions permit. This may affect the statistics later presented in Sect. 5, as dissipation may be overestimated due to the presence of these waves.

Given the extremely short time scales we are considering in our calculations (usually < 2min), we think that it is a reasonable assumption to assimilate, at the considered time scales, the increase in variance due to gravity waves to turbulent motions. Such a contamination of the strictly turbulent component of the motion from larger processes is somehow unavoidable and implicitly assumed in a variety of boundary layer calculations, for example when picking the averaging time scale to calculate Reynolds decompositions. Moreover, even when calculating turbulence dissipation rates with the traditional spectral technique from sonic anemometers, the same contamination would take place.

In the manuscript, we have made this assumption explicit as follows: “By assuming that the contribution of all atmospheric flows to the observed line-of-sight variance within the considered short time scales can be regarded as of turbulent nature, the variance σ_v^2 in (7) can be written as the sum of three different terms”.

- h) Eq. 8: In the term σ_w^2 it should be clarified that this is not the true atmospheric variation of the wind, as the smallest scales of turbulence are not resolved by the lidar.

We have modified the sentence as “ σ_w^2 is the desired net contribution from atmospheric turbulence at scales that can be measured by the lidar (Brugger et al. 2016).”

Reference: Brugger, P., Träumner, K. and Jung, C., 2016. Evaluation of a procedure to correct spatial averaging in turbulence statistics from a Doppler lidar by comparing time series with an ultrasonic anemometer. Journal of Atmospheric and Oceanic Technology, 33(10), pp.2135-2144.

- i) p. 8 line 23: Do the line-of-sight velocities need to be de-trended? Since the windows over which the variance is calculated is short (<1 min), the de-trending will effectively remove variance contributions from large eddies, especially during unstable conditions, causing an underestimate of variance (and consequently dissipation).

When using not-detrended data, the minimum error in the ϵ comparison lidar – sonics is about 10% higher than what we got with the de-trended data. Therefore, we decided to stick with the traditional (in statistics) approach of detrending time series before applying spectral analysis.

- j) p. 9 line 5: Since the sampling window is so short, measurement uncertainty/representativeness (i.e., Lenschow et al 1994) is a significant factor in the quality/error of the variance measurement as well and should be mentioned.

We have modified the sentence as follows: “In fact, the shorter the sampling time, the higher the measurement error in the estimate of the variance of line-of-sight velocity would be, because of both higher measurement uncertainty which impacts its representativeness (Lenschow et al. 1994) and a higher relative contribution of the instrumental noise.”

- k) Figure 4: Could vertical lines be added to denote the inertial subrange and/or sample length used?

We have included the following sentence in the caption of the Figure: “To calculate ϵ for these cases, the optimal sample length from comparison with the sonic anemometers corresponds to frequencies greater than $0.04s^{-1}$ for stable conditions, greater than $0.01s^{-1}$ for unstable conditions.”

- l) p. 10 line 15: Could an equation be included here for how exactly the metric presented in Fig. 5 is calculated? I assume the error is normalized by some value (as the y-axis is unitless), but this is unclear. Without this information, it is difficult to interpret Fig. 5. The caption for Fig. 5 needs to be clarified accordingly, as well.

We have added a sentence to define the metric used: “To quantify the difference between sonic and lidar estimates of ϵ , we use the median absolute error (MAE), defined as:

$$MAE = median\left(\frac{|\epsilon_{lidar} - \epsilon_{sonic}|}{\epsilon_{sonic}}\right)$$

”

We have also modified the y-axis label of the plot as “Fractional median absolute error”.

- m) p. 14 line 33: As SNR typically decreases with range, is it possible that the increase in dissipation above 600 m is due to more noisy/random errors in the line-of-sight measurements above 600 m? Thus, the increase above this height is not real (due to atmospheric turbulence), but instead due to increasing measurement errors.

A SNR threshold has been set to QC the data, however we agree that the average SNR aloft is lower, even after setting a threshold. Our data also show that we mostly had valid data aloft during high wind conditions. Therefore, we have modified the sentence as: “The slight increase of ϵ above $\sim 600m$ AGL at night for the Halo Streamline lidar can be explained as due to more random errors in the line-of-sight velocity measured by the lidar at high

altitudes but also as effect of the higher frequency of good-quality measurements at higher levels during high wind speed events”.

- n) Figure 9: The labels on these plots are small and difficult to read. Could they be made larger?

The labels are now bigger.

- o) p. 17 line 1: Are there other studies that also confirm the finding here that there is a significant gradient in dissipation right near the ground, but the changes are much smaller above 50 m? What physically results in this large almost order of magnitude change in dissipation from the surface upwards? It would be good to expand on this. Without justification or other studies that show similar results, these results seem a little suspect. Was the 5-m sonic near anything that may obstruct the flow to cause dissipation to be so large?

No obstacle was located near the 5-m sonic. We have added a reference to the sentence to show that our results are consistent with what was found in previous studies: “The plot confirms that turbulence dissipation rate shows most of its variability with height close to the surface, as also found by Balsley et al. 2006.”

We expect the increase in dissipation close to the surface to be connected with the increased TKE shear production close to the surface. Therefore, we have added the following sentence: “We expect this large reduction in ϵ to be due to a rapid decrease in shear production with height close to the surface, as it has been shown (Nilsson et al. 2016) that shear production has a strong connection with dissipation close to the surface.”

References:

- Balsley, B.B., Frehlich, R.G., Jensen, M.L. and Meillier, Y., 2006. *High-resolution in situ profiling through the stable boundary layer: examination of the SBL top in terms of minimum shear, maximum stratification, and turbulence decrease. Journal of the atmospheric sciences, 63(4), pp.1291-1307.*
- Nilsson, E., Lohou, F., Lothon, M., Pardyjak, E., Mahrt, L. and Darbieu, C., 2016. *Turbulence kinetic energy budget during the afternoon transition–Part 1: Observed surface TKE budget and boundary layer description for 10 intensive observation period days. Atmospheric Chemistry and Physics, 16(14), pp.8849-8872.*

- p) Sect 5.1: This LLJ event is atypical compared to most in the Great Plains, where the LLJ slowly reaches a wind speed maxima in the middle of the night, after which the wind speed slowly decreases. The rapid decrease in wind speed at 03 UTC seems more like there was some other disturbance (possibly on the mesoscale) that resulted in the jet diminishing. Looking at the tower data (<https://www.esrl.noaa.gov/psd/technology/bao/browser/>), there was also about a 45 degree wind shift at the time the LLJ ended. Based on surface

observation

maps

(http://www2.mmm.ucar.edu/imagearchive1/surface/ict/20150407/sfc_ict_2015040703.gif,

http://www2.mmm.ucar.edu/imagearchive1/SatSfcComposite/20150407/sat_sfc_map_2015040704.gif), there was a Denver cyclone in the area with an associated quasi-stationary front near the BAO site. Is it possible that the observed increase in dissipation was not from the LLJ itself, but is induced by a front (possibly the quasi-stationary front drifting over the site) or disturbance in the vicinity? Could a different LLJ event be chosen for this analysis? Otherwise, the text must be modified accordingly to make it clear that this observed behavior is not typical for LLJs and the presence of this quasi-stationary front likely plays a role.

We have modified the paragraph to mention the presence of the quasi-stationary front: “The analysis of the weather maps for this period reveals no frontal passage during the LLJ event, while a quasi-stationary front likely occurred at the end of the event (~04 UTC), as also confirmed by the shift in wind direction during this period, as shown in Figure 13b. No precipitation was recorded; and the analysis of ceilometer data reveals clear sky.”

However, in terms of effect on dissipation, we still think that the higher dissipation is due to the effect of the LLJ, as also pointed out in other studies (e.g. Banta et al. 2006) and found in several other LLJ events during XPIA. The shift in wind direction which corresponds to the quasi-stationary front starts at ~23LT, which determines the end of the LLJ and a rapid decrease in dissipation.

We have included the reference to the Banta et al.’s paper, as well an additional comment regarding the development of the quasi-stationary front in the following part of the section: “In correspondence to this jet, turbulence dissipation rate (Figure 13c) increases by at least an order of magnitude throughout the considered vertical portion of the boundary layer, as a consequence of an increase in wind speed variance, as observed in previous studies (Banta et al. 2006). ϵ reaches values of $\sim 10^{-2} m^2 s^{-3}$ which are comparable to what is observed during daytime convection, as can be seen between 15 and 17 LT in the presented case. This abrupt increase of ϵ , which interrupts the normal decrease of ϵ due to the transition from daytime convection to nocturnal quiescence, can also clearly be detected in the time series shown in Figure 7. After the end of the low-level jet event, in combination with the development of the quasi-stationary front, the return to more quiescent conditions, typical of the nighttime stable boundary layer, causes a considerable reduction of turbulence dissipation rate.”

Reference: Banta, R.M., Pichugina, Y.L. and Brewer, W.A., 2006. Turbulent velocity-variance profiles in the stable boundary layer generated by a nocturnal low-level jet. Journal of the atmospheric sciences, 63(11), pp.2700-2719.

Technical corrections:

a) Figure 4 caption: Should be a) after 22:15 UTC. **Corrected.**

b) p. 12 line 26: WINDCUBE is misspelled. **Corrected.**

References:

Lenschow, D. H., Mann, J., & Kristensen, L. (1994). How long is long enough when measuring fluxes and other turbulence statistics? *J. Atmos. Ocean. Tech. Technol.*, 11, 661–673.